A GENUINELY MULTIDISCIPLINARY JOURNAL

CHEMPLUSCHEM

CENTERING ON CHEMISTRY

Accepted Article

Title: Unveiling RNA Binding Properties of Verapamil and Preparation of New Derivatives as Inhibitors of HIV-1 Tat-TAR Interaction

Authors: Céline Martin, Serena De Piccoli, Marc Gaysinski, Cécile Becquart, Stéphane Azoulay, Audrey Di Giorgio, and Maria Duca

A Journal of

ChemPubSoc
Europe

WILEY-VCH   www.chempluschem.org

Unveiling RNA Binding Properties of Verapamil and Preparation of New Derivatives as Inhibitors of HIV-1 Tat-TAR Interaction

Céline Martin, Serena De Piccoli, Marc Gaysinski, Cécile Becquart, Stéphane Azoulay, Audrey Di Giorgio and Maria Duca*[a]

[a] *C. Martin, S. De Piccoli, Dr. M. Gaysinski, C. Becquart, Dr. S. Azoulay, Dr. A. Di Giorgio, Dr. M. Duca*

Université Côte d'Azur, Institute of Chemistry of Nice (ICN), 28 avenue Valrose, 06100 Nice, France

Corresponding author: maria.duca@univ-cotedazur.fr

1

Abstract

Targeting RNA using small molecules is now established as a very promising strategy for many therapeutic applications since coding and non-coding RNAs bear a pivotal role both in viral and bacterial infections as well as in human pathologies such as cancer. Here, we focused on the targeting of HIV-1 TAR RNA as a promising target for the development of new anti-HIV therapies but also as an ideal model to validate the discovery of original RNA ligands. First, we performed an initial screening of a library of compounds against TAR that led to the discovery of verapamil, a marketed calcium-channel blocker, as a promising chemical structure for the development of new RNA ligands. The synthesis of a series of analogs of verapamil led to promising structure activity relationships and to the discovery of compound **2h**, a conjugate between verapamil and indole fragment, as an efficient and selective TAR binder able to inhibit Tat/TAR interaction with an IC_{50} of 18.8 µM. This work supports the potential of library screening for the discovery of original and selective RNA ligands and illustrates how existing drugs directed against protein targets still need to be studied for RNA binding as a promising strategy in the field of RNA targeting by small molecules.

2

Introduction

Targeting biologically relevant RNAs using small-molecule drugs is becoming an important challenge for current medicinal chemistry.[1] RNA, for a long time reduced to an intermediate in the transmission of the genetic information, is now largely recognized as a major actor of important biological processes especially in the regulation of gene expression.[2] Various prokaryotic, eukaryotic and viral non-coding RNAs represent relevant targets for small-molecule ligands, peptides or oligonucleotides and recent successful examples in this field showed the feasibility of this approach.[1b, 3] While peptides and oligonucleotides may represent efficient and specific targeting tools, they often lack favorable pharmacodynamics/pharmacokinetic properties for further therapeutic applications. Targeting RNA using small molecules is thus emerging as a promising and efficient approach thanks to the fact that biologically relevant RNAs bear a three-dimensional structure offering specific binding pockets thus being much more favorable for small-molecule specific interaction compared to double helical DNA.[1d] Indeed, RNA is a major target for various classes of antimicrobial drugs, such as aminoglycosides, tetracyclines or oxazolidinones that are able to selectively bind to prokaryotic ribosomal RNA thus impairing protein synthesis in bacteria.[4] Its role in RNA viruses is also largely recognized thus rendering viral RNAs potential targets for innovative therapies.[5]

In this context, a potential target for the development of new antiviral therapies is represented by the HIV-1 transactivation response (TAR) element. This RNA fragment binds to the Tat protein and is essential for efficient human immunodeficiency virus (HIV) replication (Figure 1A).[5-6] This RNA is constituted by 59 nucleosides located in the 3'-UTR of each viral transcript and spontaneously generates a stem-loop structure.[7] TAR RNA interacts with the viral protein Tat and with positive transcription elongation factor b (P-TEFb) itself constituted by cyclin T1 and cyclin-dependent kinase 9 (CDK9), thus controlling transcription. The interaction between Tat and TAR is mediated by an arginine-rich region that recognizes the bulged region of TAR.[8] The inhibition of Tat/TAR interaction should thus induce the inhibition of viral replication and a various RNA binders able to block this interaction have been reported.[6] TAR RNA thus represents particularly relevant model system to study ligand binding to RNA as well as a promising target for the discovery of compounds with anti-HIV activity.[9]

During recent years, various small-molecule RNA binders able to target biologically relevant RNAs have been identified.[1a, 1c, 10] One major example is represented by RNA-interacting compounds acting as pre-mRNA splicing modifiers of SMN2 (survival motor neuron 2 protein). Some of these ligands recently found clinical application in the treatment of Spinal Muscular Atrophy (SMA).[11] Very specific RNA binders targeting the production of oncogenic microRNAs in cancer cells and *in vivo* have also been reported.[12] In this case, an approach called InfoRNA was developed to identify lead binders using a statistical prediction of compounds affinity and selectivity based on a previous screening of a large library of compounds against a library of RNA motifs.[13] This allowed for the discovery of compounds

3

bearing an exceptional specificity for miR-96 precursor or for miR-210 precursor both in cells and in animals models.[10a, 12c]

We also discovered various RNA ligands upon combination of different RNA binding domains carefully selected to bring both affinity and selectivity for the target.[14] For example, we conjugated artificial nucleobases, that are able to interact selectively with RNA base pairs, with basic amino acids that can bring affinity for an efficient targeting of TAR RNA *in vitro* and in infected cells.[15] A similar approach was used for the preparation of *C*-nucleosides targeting prokaryotic A-site RNA.[16] We also conjugated known antibiotics, such as aminoglycosides, with artificial nucleobases and amino acids leading to multimodal RNA ligands able to selectively target oncogenic miRNAs *in vitro* and in cancer cells overexpressing these miRNAs.[14a] Concomitantly to the focused design of new RNA ligands, we performed screening of larger libraries of compounds against oncogenic miRNAs.[17] This led to the identification of an array of chemical scaffolds bearing favorable properties in terms of binding and selectivity *in vitro* but also inside cancer cells.

Here, we describe the screening of an in-house library of commercial compounds that allowed for the identification of verapamil, a phenylalkylamine calcium channel blocker currently in clinical use as an antiarrhythmic compound (Figure 1B), as a potential scaffold for the preparation of new RNA ligands. As mentioned above, the conjugation of RNA ligands with other RNA binding domains led to promising and selective RNA binders. We thus decided to prepare a reduced form of verapamil and to conjugate it with fragments identified as RNA binders during the screening of the library and with known RNA-binding moieties led to the preparation of a series of verapamil analogs and to the improvement of TAR RNA affinity and selectivity. Noteworthy, the conjugation of verapamil to an indole fragment through reductive amination led to a compound (**2h**) which is able to efficiently inhibit Tat/TAR interaction *in vitro* with 18.8 μM IC$_{50}$. This represents a very promising inhibition activity compared to small-molecule RNA ligands already reported in the literature.[9, 18] The detailed study of the molecular mechanism of interaction of **2h** with TAR RNA led to important insights about the chemical features that are relevant for binding and for the design of future efficient TAR binders and potential antiviral compounds. Verapamil has never been considered for RNA binding and this work represents the first example of verapamil chemical modification applied to RNA targeting thus opening new perspectives in the RNA targeting field.

Results and discussion

Library screening. The library of compounds and fragments chosen for this study belongs to an in-house collection of commercial compounds and contains 188 molecules (see Table S1 in the Supporting Information for the complete list) whose 90% can be considered as fragments (MW < 300, ClogP, H-bond donors and acceptors and n° of rotatable bonds < 3).[19] The remaining 10% are molecules bearing higher molecular weight but that could present an interest as scaffolds for the preparation of new RNA binders. We also decided to add to this library some antibiotics that are efficient and non-selective RNA

4

binders, such as aminoglycosides and tetracyclines that could function as positive controls. The aim of the initial screening was to identify compounds bearing even modest affinity for TAR RNA in order to later improve their binding and biological activity upon chemical modification as usually performed in a fragment-based approach. Hits growing (addition of substituents) and linking (combination with other hits) could lead indeed to relevant improvements of affinity and of selectivity allowing for the discovery of new scaffolds and for the design of RNA ligands with potential antiviral activity.

First, we screened the library measuring the affinity toward a 27-mer TAR fragment labeled in 5′ position with Alexa[488]. This kind of fluorescence-based assay relies on the fact that binding of an efficient ligand to the labeled target induces a change in fluorescence intensity that is dependent on the concentration of ligand and it has been largely validated in the literature.[20] We screened fragments at 10 μM and 100 μM leading to the identification of 9 compounds showing affinity (at least 20% fluorescence variation) at both concentrations (guanine, thioguanine, phenothiazine, neomycin, oxytetracycline, 1,6-dibromo-2-hydroxynaphthalene-3-carboxylic acid, cinchonidine, verapamil and apramycin, Figure S1) and 9 compounds showing some affinity only at 100 μM concentration (2-aminobenzimidazole, 5-aminomethylindole, 2-aminothiazole, 3,5-dibromosalycilic acid, 3,5-dichlorosalycilic acid, 3-acetylindole, 4-dimethylamino benzaldehyde, 2,6-diaminopurine and puromycin, Figure S2). Among the strongest binders, neomycin, oxytetracycline, apramycin and puromycin are known RNA binders able to bind prokaryotic ribosomal RNA and impair protein synthesis in bacteria. Phenothiazine, cinchonidine and naphthalene derivative are known intercalating agents and have been previously studied for RNA binding.[21] Purines, such as guanine and thioguanine have also been studied as RNA binding motifs.[14c, 22] The remaining compound, verapamil, revealed to have interesting affinity for TAR and this pharmacophore has never been explored for RNA binding. It thus seemed an appropriate starting point for the development of new and original RNA ligands. Indeed, verapamil is a calcium channel blocker currently used clinically for the treatment of arrhythmia and other cardiovascular pathologies.[23] We thus decided to take advantage of verapamil to synthesize conjugates with other scaffolds identified during the initial screening (namely phenothiazine, naphthalene, quinolone, benzimidazole, indole, thiazole, 3,5-dibromo-salicilic acid and 4-dimethylaminobenzaldehyde) as well as with known RNA binding domains (such as benzothiazole, phenylthiazole, imidazole and amino acids lysine, histidine, phenylalanine and arginine).

Synthesis of a new series of verapamil analogs. In order to conjugate verapamil to other RNA-binding motifs, we first chose to reduce verapamil nitrile group using LiAlH$_4$ in THF to obtain desired amine-containing compound **1** in 96% yield as previously reported in the literature (Scheme 1).[23] Starting from this compound, we chose three different functionalization routes: (i) reductive amination upon reaction with aldehydes (Scheme 1), (ii) amide formation upon reaction with carboxylic acids (Scheme 2) and (iii) introduction of a carboxyl group on verapamil using succinic anhydride followed by amide formation upon reaction with amines (Scheme 3).

5

Regarding the reductive amination reaction, we chose to react **1** with aldehyde-containing compounds that demonstrated to have some affinity during fragment screening (Scheme 1): 4-dimethylaminobenzaldehyde (as in **2a**), 1-naphthaldehyde (as in **2b**), 3,5-dibromo-2-hydroxybenzaldehyde (as in **2c**), 4-quinolinecarboxaldehyde (as in **2d**), *N*-Boc-3-formyl-1*H*-indole-1-carboxylate (as in **2'h**). Beside these five aldehyde compounds, we also chose four different heterocyclic moieties containing an aldehyde group and known as interesting moieties for RNA targeting[10c]: benzothiazole (as in **2e**), phenylthiazole (as in **2f**), thiazole (as in **2g**) and *N*-Boc-indoline (as in **2'i**). Reductive amination in the presence of these aldehydes was performed using classical conditions (NaBH$_3$CN in CH$_2$Cl$_2$/MeOH 50:50) and led to the formation of compounds **2a-g** and **2'h-2'i** in 52-68% yields. Compounds **2'h** and **2'i** containing a Boc protecting group were further deprotected in the presence of TFA in CH$_2$Cl$_2$ leading to **2h** and **2i** in 94% and 78% yields, respectively.

For the preparation of analogs bearing an amide linkage between verapamil and the modifying moiety, we chose two different strategies. The first one is the direct coupling of carboxylic acids on the amino group of compound **1** (Scheme 2). In this case, we also took advantage of chemical moieties identified during the screening process by coupling 4-dimethylaminobenzoic acid (as in **3a**), 10*H*-phenothiazine-10-carboxylic acid (as in **3b**), benzoic acid (as in **3c**), 2-thiophenecarboxylic acid (as in **3d**) and 4-*N*-tert-butoxycarbonyl-aminobenzoic acid (as in **3e**). We also conjugated **1** with *N*α,*N*ε-di-Boc-L-lysine (as in **3'f**), *N*α,*N*im-di-Boc-L-histidine (as in **3'g**), *N*α-Boc-L-phenylalanine (as in **3'h**) and *N*α-Boc-*N*γ-(4-methoxy-2,3,6-trimethylbenzenesulfonyl)-L-arginine (as in **3'i**). Amino acids are indeed RNA binding agents as they constitute natural RNA ligands, i.e. peptides. Peptide coupling between compound **1** and these carboxylic acids in the presence of HOBt, EDC and Et$_3$N in CH$_2$Cl$_2$ led to the formation of compounds **3a-d** and **3'e-3'i** in 56-86% yields. Compounds **3'e-3'h** containing a Boc group were deprotected in the presence of TFA in CH$_2$Cl$_2$ leading to desired products **3e-3h** in 79-95% yields. Compound **3'i** containing a Mtr and a Boc protecting groups was first deprotected on the *N*α in the presence of TFA in CH$_2$Cl$_2$ then treated with a solution of phenol/TFA 5% w/w to remove the Mtr group of *N*γ. These two steps led to **3i** in 95% yield.

Finally, compound **1** was modified with the introduction of a succinamic acid side chain that was introduced upon reaction of **1** with succinic anhydride in CH$_2$Cl$_2$ leading to compound **4** in 95% yield (Scheme 3). **4** was then coupled with compound **1** to form a verapamil dimer (as in compound **5a**) as well as with 2-aminothiazole (as in compound **5b**) in the presence of HOBt, EDC, Et$_3$N in CH$_2$Cl$_2$ leading to desired compounds **5a** and **5b** and **5'c** in 27% and 25% yield, respectively. Compound **4** was also coupled with *N*-Boc-2-aminobenzimidazole (as in compound **5'c**) in the presence of HBTU and DIPEA in CH$_2$Cl$_2$ leading to a mixture of **5'c** and **5c**. Addition of TFA in CH$_2$Cl$_2$ led to desired compound **5c** in 25% yield over two steps.

All synthesized compounds were characterized by NMR, HRMS and ultimately purity was verified by HPLC before their biological evaluation.

6

Evaluation of binding affinity and selectivity of the newly synthesized verapamil analogs. All synthesized compounds **2a-i**, **3a-i** and **5a-c** were evaluated as TAR RNA binders using the same fluorescence-based assay that was employed for the initial screening but performing this assay over a range of ligands concentrations. Compounds **1** (reduced verapamil) and **4** (verapamil conjugated to the succinamic acid linker) as well as all moieties that were employed for conjugates synthesis were used as controls. The measurement of fluorescence variation as a function of compounds concentration led to the calculation of dissociation constants (K_D) as reported in Figure 2. First of all, while verapamil showed a $K_D > 100$ μM that could not be measured precisely, compound **1** bears a K_D of 3.2 μM demonstrating a strong improvement of the affinity for the target once the nitrile group is reduced. Reductive amination products **2a-2i** were the most promising TAR binders with K_D in the low micromolar range from 0.66 μM for **2e**, 0.71 and 0.72 μM for **2i** and **2h**, respectively, until 22.1 μM for **2c**. Amide formation products **3a-3i** were globally less strong binders except **3f**, **3g** and **3i** that showed a submicromolar K_D (0.41 μM, 0.45 μM and 0.63 μM, respectively). Finally, amide formation products **5a-5c** showed weak affinity with 12.9 μM K_D for **5a** and no measurable binding for **5b** and **5c**. These results demonstrated that benzothiazole, indole and indoline as in **2e**, **2h**, **2i** as well as basic amino acids lysine, histidine and arginine as in **3f**, **3g** and **3i** are more favorable for binding once conjugated to verapamil with K_D values in the submicromolar range. 4-dimethylaminophenyl, naphthalene, quinolein and phenylthiazole moieties as in **2a**, **2b**, **2d**, **2f** and **3h** keep affinity for the target with K_D in the low micromolar range but globally loose affinity compared to the first group of ligands. Compounds **2g**, **3b**, **3c** and **3d** bearing thiazole, phenothiazine, phenyl and thiophene substituents, respectively, showed only low affinity with K_D over 10 μM. Finally, compounds **2g**, **3a**, **3e**, **5b** and **5c** bearing thiazole (conjugated *via* amide formation as in **2g** and **5b**), 4-dimethylaminophenyl (conjugated via amide formation), 4-aminophenyl and benzimidazole showed no affinity for the target. It is important to note that all moieties tested without conjugation with verapamil showed very low affinity for the target and a K_D value could not be measured in the tested range of concentrations.

Affinity measurements alone are not representative of the potential of an RNA ligand, since a lack of selectivity could hamper the biological activity. In order to appreciate the selectivity of each compound we decided to measure K_D values in the presence of a large excess of competitors such as tRNA and DNA (100 eq. of each competitor). As illustrated in Figure 2, these experiments allowed us to discriminate the most selective compounds. While **1**, **2a-b**, **2e-f**, **2h-i**, **3f-i** and **5a** retained affinity in the presence of tRNA, only compounds **1**, **2h**, **3f** and **3i** retained TAR RNA affinity in the presence of DNA. This suggested that these latter were much more favorable for future studies keeping in mind that **2h**, **3f** and **3i** are also the strongest binders.

Based on these results, we analyzed the thermodynamic features of the interactions of the most promising compounds **2h**, **3f** and **3i** in comparison with parent compound **1** as well as compound **2a** both being good but non-selective ligands and the results are as summarized in Table 1.[24] Free energies of Gibbs (ΔG°) were first calculated from the dissociation constants ($ΔG° = -RT \ln K_D$) for all

7

compounds and found to be very similar (from −30.0 to −36.5 kJ/mol). To complete the thermodynamic binding profiles, the enthalpic (ΔH°) and the entropic (−TΔS°) energy contributions were determined after the determination of $\Delta G°_T$ at several temperatures (278−308 K). In all cases, the interaction is driven by the enthalpy suggesting the formation of specific interactions, such as hydrogen bonds, with the RNA target. In compounds **2h** and **3f**, the entropic contribution is close to zero while for compounds **2a** and **3i** its relevance is more important suggesting that electrostatic interactions and desolvation probably contribute to binding of these latter compounds. Furthermore, the total energy represented by the ΔG° value is composed of two components: (i) the first one reflects the non-electrostatic interactions (nonionic hydrophobic effects driven by entropy, specific interactions, including H-bonds, van der Waals interactions, and π-stacking) that contribute to the total free nergy ($\Delta G°_{nel}$ value) and ii) the pure electrostatic contribution given by ionic interactions occurring between two groups of opposite charge ($\Delta G°_{el}$ value) that can be highly dependent on the salt concentration. As suggested by the enthalpy values, $\Delta G°_{nel}$ is over 90% for all compounds with **2h** showing 99% of non-electrostatic interactions formed. Altogether, binding studies demonstrated that various compounds are good RNA binders, but only few conjugates are selective for TAR and that compound **2h**, conjugate between verapamil and indole using reductive amination, is the best and most selective ligand.

Inhibition of TAT/Tar interaction. Once identified the strongest and most selective binders, namely compound **2h** followed by **1**, **3f** and **3i**, we wondered if these ligands could be able to inhibit Tat/TAR interaction *in vitro* and we compared their efficacy with compound **2a**. The ability of these compounds to displace a Tat fragment from a preformed TAR/Tat complex was assessed *via* a FRET assay, developed from a previously described procedure,[25] using a fluoresceinated Tat peptide fragment (amino acids 48–57) and a Dabcyl-labeled TAR fragment (nucleotides 18–44). In the absence of ligand, association of these two partners results in an efficient quenching of the dyes. Upon addition of increasing amounts of compounds **1**, **2a**, **2h**, **3f** and **3i**, the fluorescence rises in almost all cases, demonstrating that these ligands can displace the Tat fragment from a preformed Tat/TAR complex. IC_{50} values associated with each compound are given in Table 1. These experiments showed that reduced verapamil (**1**) and compound **2a** were not efficient inhibitors of Tat/TAR interaction with IC_{50} of 1.87 mM for 1 and no inhibition for **2a** and that all other ligands were able to inhibit the formation of the complex with micromolar IC_{50}. Compounds **3f** and **3i** showed an IC_{50} of 302 μM and 404 μM, respectively, further confirming the potential of basic amino acids lysine and arginine for the preparation of RNA binders as previously reported. The best TAR ligand **2h** showed an IC_{50} of 18.8 μM thus demonstrating to be not only the strongest and most selective ligand but also the most efficient inhibitor of Tat/TAR interaction. This results further underlines how inhibition studies are essential for the identification of the most promising binders since dissociation constants alone do not allow the discrimination between equally efficient ligands. All *in vitro* studies converged to the demonstration that reduced verapamil conjugated to an indole *via* reductive amination, as in compound **2h**, led to the

8

best binding features and *in vitro* activity thus suggesting that the mode of binding and the site of interaction of **2h** is particularly favorable for inhibition and deserved to be studied more in detail.

Evaluation of the molecular mechanism of interaction. In order to study more in detail the molecular mechanism of interaction of compound **2h** with TAR, we decided to identify which residues were affected upon binding in comparison to non-modified parent compound **1**. NMR spectroscopy was thus employed to examine the structure of HIV-1 TAR RNA in both ligand-bound and free states. Therefore, following the changes in chemical shifts of TAR as a ligand is titrated into solution provides an indication of how the ligand interacts with TAR. Upon titration of **1** into TAR, the most significant chemical shifts changes were observed for residues in the bulge area of TAR (Figure 3), confirming that verapamil specifically interacts with this bulge. The most affected residues are located between U23 and G26 as well as between U38 and U40. Titration of **2h** leads to similar chemical-shift changes but two important differences were observed: (i) the interaction with TAR is extended to more residues since the strongest variations are observed from U23 to G26 and between C37 and U42 and (ii) G26 chemical shift is particularly modified by **2h** with 0.3 ppm variation *versus* 0.05 ppm for **1**. This demonstrates that the binding site of **1** and **2h** remains the same before and after conjugation but that further interactions are formed with the target by the additional moiety thus reinforcing the interaction and rendering it more efficient in terms of selectivity and inhibition activity. Interestingly, other compounds of the series that showed good affinity do not show the same level of inhibition. As an example, compound **2a**, containing a dimethylaminophenyl substituent conjugated upon reductive amination, bears a K_D of 1.3 μM but no inhibition of Tat/TAR interaction. Indeed, the NMR study of its site of interaction (Figure S7) confirmed that this kind of chemical modification induces a different binding site compared to **1** and **2h**. In fact, G26 is not affected by **2a** while residues from U38 to U42 are only slightly shifted.

Confirmation of these results came from molecular docking that we performed using AutoDock 4. We employed a flexible ligand and TAR receptor to calculate independent docking events utilizing a Lamarckian genetic algorithm and selected the 10 docking poses bearing the lowest energy in the presence of compounds **1** and **2h**. As illustrated in Figure 4, docking suggested that the interaction of both compounds occurs at the level of the bulge site. The obtained results suggested the formation of H-bonds and electrostatic interactions with phosphates and bases located in the region between G21 and U25 as well as between C41 and U42 in the case of compound **1** (Figure 4A). Molecular docking is also consistent with the formation of more specific hydrophobic interactions between the indole moiety and G26 as well as various H-bonds with U26-A27 and U40-C41 in the case of **2h** (Figure 4B). The comparison of these results with the molecular docking of compound **2a** (Figure S8) suggested that this latter interacts more specifically with the stem region with residues G17 and C19 as well as with residues U38, C39, U40 and U42 as suggested by NMR studies. **2a** thus seems to interact in a very different manner compared to **1** and **2h** further demonstrating that the site of interaction is extremely important for an efficient inhibition of RNA interaction with its biological partners. i.e. TAR interaction with Tat

9

peptide. Indole moiety forms additional hydrophobic interactions with residue G26 as well as hydrogen bonds with U40 and C41 thus increasing the strength and the number of interactions and improving the selectivity and the inhibition activity. Efficient and selective binding at a particular site of the target is thus essential to have good inhibition activity as demonstrated by the comparison of **2h** with **2a**.

Conclusion. The screening of a library of commercially available compounds for their ability to bind HIV-1 TAR RNA led to the discovery of a small number of hits and in particular to the identification of verapamil, a phenylalkylamine calcium channel blocker currently in clinical use as an antiarrhythmic compound, as a promising scaffold for the preparation of new RNA binders. Verapamil has never been studied as an RNA ligand and we chose it for the synthesis of a new series of RNA ligands obtained upon conjugation of verapamil to other hits identified during screening or other known RNA-binding motifs. This led to the synthesis of 21 new compounds. Some of these compounds demonstrated to be very good TAR binders and ligands **2h**, **3f** and **3i** also showed selectivity in the presence of a large excess of both tRNA and DNA. **2h**, where indole fragment was coupled to verapamil, was the most efficient inhibitor of Tat/TAR interaction with an IC$_{50}$ of 18.8 μM and the detailed study of its molecular mechanism of interaction demonstrated that this compound binds to the bulge site of TAR efficiently and selectively thus being a promising hit for future optimization.

Drug discovery in the field of RNA targeting is an interesting challenge for medicinal chemistry with great potential for future therapies. Library screening showed to be an efficient approach for the discovery of new RNA ligands bearing biological activity. Here, we thus described a screening that led to the discovery of verapamil, a drug currently employed in the treatment of some cardiovascular diseases, as an efficient TAR RNA binding agent. The chemical modification of this marketed drug showed that the biological activity can be greatly improved thus leading to strong and selective binders of HIV-1 TAR RNA. Even if the most active and selective compound **2h** needs further optimization before antiviral studies in infected cells, this work demonstrated that the study of existing drugs as scaffolds for the preparation of efficient RNA ligands could be an interesting strategy toward original ligands in the field of RNA targeting by small molecules.

Experimental section

Chemistry

Materials. Reagents and solvents were purchased from Merck and Carlo Erba Reagents and used without further purification. All reactions involving air- or moisture-sensitive reagents or intermediates were performed under an argon atmosphere. Flash column chromatography was carried out on silica gel columns (Interchim Puriflash silica HP 15 μm) on a Puriflash XS420 system (Interchim). Analytical thin-layer chromatography (TLC) was conducted on Sigma Aldrich precoated silica gel and compounds were visualized by irradiation (254 nm) and/or by staining with ninhydrin and phosphomolybdic acid. HPLC was performed using a Water Alliance 2695 pump coupled with Waters 996 photodiode array detector and a Waters XSELECT™ CSH™ Fluoro-Phenyl (2.5 μm, 4.6x150 mm ColumnXP for

10

analytical HPLC and 10 x 150 mm for semipreparative HPLC). All HPLC analyses were run at room temperature using a gradient of CH₃CN containing 0.1% TFA (eluent B) and water containing 0.1% TFA (eluent A) from 5% to 100% of B in 30 min at a flow rate of 1 mL/min for the analytical column and 3.5 mL/min for the semipreparative column. ¹H and ¹³C NMR spectra were recorded on a Bruker AC 200 MHz or a Bruker AC 400 MHz spectrometer. Chemical shifts are reported in parts per million (ppm, δ) referenced to the residual ¹H resonance of the solvent (CDCl₃, δ 7.26; CD₃OD δ 3.31; DMSO-d_6 δ 2.50). Splitting patterns are designated as follows: s (singlet), d (doublet), t (triplet), m (multiplet), br (broad). Coupling constants (J values) are listed in hertz (Hz). Low resolution mass spectra (MS) were obtained with a Brucker Daltonics Esquire 3000+ electrospray spectrometer equipped with API ionization source. High resolution mass spectra (HRMS) were obtained with a LTQ Orbitrap hybrid mass spectrometer with an electrospray ionization probe (Thermoscientific, San Jose, CA) by direct infusion from a pump syringe to confirm correct molar mass and high purity of compounds.

General procedure for reductive amination (General procedure A). To a solution of 1.3 eq. of the appropriate aldehyde (0.15 mmol) in CH₂Cl₂ or CH₂Cl₂/MeOH (1:1) (4 mL) is added 1 eq. of compound **1** (50 mg, 0.11 mmol). When necessary the pH is adjusted to pH=5-6 by addition of acetic acid. Then NaBH₃CN (14 mg, 0.22 mmol, 2 eq.) is added and the reaction mixture is stirred at room temperature overnight. The solvent is then removed under reduced pressure. CH₂Cl₂ is added to the crude product and the organic phase is washed with a solution of NaHCO₃ (10%), water and brine. After drying over MgSO₄ and filtration, the solvent is evaporated under reduced pressure and the residue is purified by flash chromatography on a silica gel column using a gradient of CH₂Cl₂/MeOH 9:1 as the eluent.

(±)-5-[(3,4-Dimethoxyphenethyl)methylamino]-2-(3,4-dimethoxyphenyl)-2-isopropylpentyl-*N*1-(tert-butyl-1*H*-indolecarboxylate-3-methyl)amine (2'h).

Compound **2'h** was prepared following general procedure A in the presence of *tert*-butyl 3-formyl-1*H*-indole-1-carboxylate (36 mg). Compound **2'h** was obtained as a yellow solid: 44 mg (59%); R_f = 0.25 (CH₂Cl₂/MeOH 95:5); ¹H NMR (400 MHz, CD₃OD) δ = 8.09 (d, *J*=8.2 Hz, 1H), 7.59 (d, *J*=7.7 Hz, 1H), 7.56 (s, 1H), 7.31-7.15 (m, 2H), 6.86-6.76 (m, 4H), 6.74 (d, *J*=1.9 Hz, 1H), 6.66 (dd, *J*=8.1, 1.9 Hz, 1H), 3.94 (d, *J*=13.7 Hz, 1H), 3.89 (d, *J*=14.1 Hz, 1H), 3.80-3.74 (m, 9H), 3.68 (s, 3H), 3.07-2.97 (m, 2H), 2.71-2.58 (m, 4H), 2.48 (t, *J*=7.6 Hz, 2H), 2.26 (s, 3H), 1.99-1.91 (m, 1H), 1.86-1.77 (m, 2H), 1.65 (s, 9H), 1.46-1.26 (m, 2H), 0.76, 0.71 (2d, *J*=6.8 Hz, 6H); ¹³C NMR (101 MHz, CD₃OD) δ = 151.0, 150.5, 149.8, 149.0, 148.8, 137.1, 136.7, 133.6, 131.6, 125.5, 125.1, 123.7, 122.0, 121.7, 120.6, 120.4, 116.2, 113.7, 113.5, 113.2, 112.3, 84.9, 59.9, 58.8, 56.6, 56.5, 56.4, 56.4, 53.7, 47.8, 45.6, 42.3, 35.3, 33.0, 32.2, 28.4, 22.1, 18.5, 18.4; MS (ESI): *m/z* 688.27 (M+H)⁺ (theoretical 688.42).

(±)-5-[(3,4-Dimethoxyphenethyl)methylamino]-2-(3,4-dimethoxyphenyl)-2-isopropylpentyl-*N*1-(1*H*-indole-3-methyl)amine (2h).

Compound **2h** was dissolved in CH₂Cl₂ (3 mL) and TFA (195 μL; 2.55 mmol, 40 eq.) was added. The reaction mixture was stirred at 35 °C for 3 hours. The solvent was removed under reduce pressure. The crude product was then triturated with Et₂O and after filtration, **5b** was obtained as a brown solid: 35

11

mg (94%); R_f = 0.3 (CH$_2$Cl$_2$/MeOH 93:7); ^{1}H NMR (400 MHz, CD$_3$OD) δ = 7.79 (d, J=7.8 Hz, 1H, *h*), 7.55 (s, 1H), 7.47 (d, J=8.0 Hz, 1H), 7.25-7.13 (m, 2H), 6.92-6.85 (m, 2H), 6.82-6.72 (m, 2H), 6.55-6.46 (m, 2H), 4.56 (d, J=14.0 Hz, 1H), 4.49 (d, J=13.9 Hz, 1H), 3.84-3.73 (m, 9H), 3.63-3.51 (m, 5H), 3.32-3.05 (m, 4H), 3.04-2.87 (m, 2H), 2.79 (s, 3H), 2.08-1.73 (m, 3H), 1.61-1.43 (m, 2H), 0.71, 0.55 (2d, J=6.7 Hz, 3H); ^{13}C NMR (101 MHz, CD$_3$OD) δ = 150.8, 150.2, 149.8, 149.8, 138.0, 131.6, 130.1, 129.4, 128.8, 123.6, 122.3, 121.6, 121.5, 119.0, 113.7, 113.4, 113.2, 112.8, 112.6, 104.89, 58.4, 57.2, 56.5, 56.5, 56.3, 50.0, 46.9, 44.0, 40.5, 34.3, 31.0, 30.3, 19.8, 17.9, 17.7; HRMS (ESI): *m/z* 588.37988 (M+H)$^+$ (C$_{36}$H$_{50}$N$_3$O$_4$ requires 588.37958).

NMR experiments

Materials and equipment

NMR experiments were conducted as described in a previous work and detailed below.[26] High resolution NMR experiments were recorder on a BRUKER AVANCE Ultra shield DRX 500 spectrometer operating at 500.13 MHz for 1H, equipped with a temperature control unit (BCU 6.0, BVT 3000), and an inverse probe head (5mm PHTXI 1H-13C/15N Z-GRD). Proton chemical shift was referenced internally by setting the carrier frequency on water at the center of the spectrum (4.71ppm at 13°C and 4.70ppm at 35°C). Chemical shifts (δ) are expressed in parts per million (ppm). All NMR experiments were carried out using standard pulse sequences supplied by the spectrometer manufacturer (BRUKER). 1D and 2D spectra were processed using TOPSPIN 2.1 NMR Software (BRUKER).

For the preparation of all NMR samples, a folding of TAR RNA (100 μM) was performed in the appropriate buffer (vide infra) as described in material and methods section of the paper. After refolding, the NMR sample (alone or with the appropriate amount of ligand) is incorporated into a Shigemi NMR tube.

^{1}H NMR imino proton spectra were recorded in a H$_2$O/D$_2$0 (90/10) buffer containing 20 mM phosphate and 50 mM NaCl at 286°K (13°C) by using a WATERGATE 3-9-19 water suppression. Each proton NMR spectrum was acquired using 10.964 KHz Spectral Width (SW), 64K complex data point, acquisition time (aq) of 2.98 s, relaxation delay (D1) of 1s, number of scan (ns) between 1000 and 2000, number of dummy scan (ds) 4 and a 90° flip angle pulse width. Water suppression was achieved using WATERGATE pulse sequence. Gradient pulse were sine shape (SINE.100), 1.5 ms long (P16) with 100 μs gradient recovery delay (D16) and strengths set to 8.44 Gauss.cm-1 (20%). A 45.6 μs delay (D19) was used for binomial water suppression. Prior to Fourier transformation, the fids were multiplied by an exponential line broadening function of 3 Hz.

gs-TOCSY Phase sensitive (States – TPPI mode) experiments using MLEV 17 pulse sequence for spin lock were recorded in a D20 buffer (50 mM NaCl, 20 mM phosphate, pH 7.4) at 308K (35°C) by using a WATERGATE 3-9-19 water suppression. Each TOCSY 2D NMR spectrum was acquired with a spectral width of 5 KHz in both dimension, 2K complex data point in F2, 256 t1 increments (between 32 and 64 scans by increment) in F1, 0.20 s for aq and D1 of 2 s. MLEV 17 pulse sequence for spin lock was set to 60 ms. Water suppression was achieved using WATERGATE pulse sequence. Gradient

12

pulse were sine shape (SINE.100), 1.5 ms long (P16) with 100 µs gradient recovery delay (D16) and strengths set to 8.44 Gauss.cm-1 (20%). A 100 µs delay (D19) was used for binomial water suppression. Prior to Fourier transformation a QSINE window function (SSB =2) was applied in both dimension and the data were zero filled and linear predicted (NC=32) to 1K data points in F1.

Molecular Modeling and Docking. The experimental structure of RNA TAR complexed with ligand rbt158 (pdb code 1UUI) was used as input for our calculations. As described in our previous work,[27] for docking with AutoDock, polar hydrogen atoms, Kollman united charges and solvent parameters were applied to the RNA using pmol2q script (http://www.sourcefiles.org/Scientific/Biology/Proteins/pmol2q_2.3.0.tar.gz). This script converts the .pdb file format to of the RNA template to the .pdbqt file format that is compatible with AutoDock program version 4 (http://autodock.scripps.edu/). The compounds .pdbqt files compatible with Autodock program version 4 were prepared from the .pdb files obtained from http://ligand-expo.rcsb.org/ (NMY).

RNA-ligand molecular dockings were conducted using AutoDock program version 4. The rotational bonds of the ligand were treated as flexible, whereas the receptor was kept rigid. Grid box was fixed in order to include the entire RNA sequence. RNA-ligand interactions were analyzed and visualized using Discovery Studio Visualizer version 4.1 (http://accelrys.com/products/discovery-studio/).

Biochemistry

Unless otherwise stated, all reagents and solvents were of analytical grade and from Sigma (St Louis, U.S.A.). HEPES and all inorganic salts for buffers were purchased from Merck (molecular biology grade). RNA and DNA oligonucleotides were purchased from IBA GmbH and used without further purification. Oligonucleotide sequences: TAR (5'-Alexa488-CCAGGUCUGAGCCUGGGAGCUCCCUGG-3'), DNA (5'-CGTTTTTATTTTTGC-3' and 5'-GCAAAAATAAAAACG-3'). A mixture of pre- and mature yeast tRNAs (containing over 30 different species) was purchased from Sigma (type X-SA). Stocks of tRNAmix can be quantified in its native form (without base hydrolysis) using an extinction coefficient of 9640 cm-1 M-1 per base.

Buffers: All buffers were filtered through 0.22 µm Millipore filters (GP ExpressPLUS membrane). A small aliquot (100 mL) was first filtered and then discarded to avoid any contaminants that might be leached from the filter. The solutions to be used in the fluorescence experiments were prepared by diluting the concentrated stocks in Milli-Q water and filtered again as described above. All standard fluorescence measurements were performed in buffer A (20 mM HEPES (pH 7.4 at 25°C), 20 mM NaCl, 140 mM KCl and 3 mM $MgCl_2$). FRET experiments were performed in buffer B (50mM tris buffer (pH 7.4 at 25°C), 20 mM KCl and 0.005% Tween 20). For competitive experiments in the presence of a tRNA, a mixture of pre- and mature yeast tRNAs (containing over 30 different species from baker's yeast *(S. cerevisiae*, Sigma, type X-SA)) was added to buffer A to obtain a 100-fold nucleotide excess regarding TAR RNA.

13

Inhibition of Tat/TAR interaction. As previously described,[28] Ligand solutions and RNA (40 nM working solution) were prepared as described above in buffer B (50mM tris buffer (pH 7.4 at 25°C), 20 mM KCl and 0.005% Tween 20). Labeled Tat peptide was prepared at 40 nM in buffer B and mixed to an equal volume of TAR RNA for 20 min at room temperature to form the Tat/TAR complex before adding the ligand. The appropriate ligand solution (30 μL) was then added to a well of a non-treated black 384-well plate, in triplicate, and 30 μL of the Tat/TAR solution was added. This subsequent dilution lowered the final Tat/TAR concentration to 10 nM. Fluorescence was measured as described above after 30 min of incubation at room temperature.

Binding studies: Ligand solutions were prepared as serial dilutions in buffer A at a concentration four times higher than the desired final concentration to allow for the subsequent dilution during the addition of the RNA solution. Binding experiments were performed in 384-well plates (Greiner bio-one) in a final volume of 60 μL using a 5070 EpMotion automated pipetting system (Eppendorf). Each experiment was performed in duplicate. 10 nM TAR beacon was used in each well. Each ligand was added in 15 dilutions (from 0.030 nM to 0.5 μM) and the fluorescence increase measured after 4 hours. The fluorescence was measured on a GeniosPro (Tecan) with an excitation filter of 485±10 nm and an emission filter of 535±15 nm. Each point was measured 10 times with a 500 μs integration time and averaged. Binding data were analyzed using Graphpad Prism 5 software. Unless otherwise stated, binding profiles were well modeled using a simple model assuming the one to one stoichiometry. Refolding of the RNA was performed using a thermocycler (ThermoStat Plus Eppendorf) as follow: the RNA, diluted in 1 mL of buffer A at a concentration of 200 nM, was first denatured by heating to 90°C for 2 min, then cooled to 4°C for 10 min followed by incubation at 20°C for 15 min. After refolding, the RNA was diluted to a working concentration of 10 nM through addition of the appropriate amount of buffer A. The tube was mixed and 50 μL of the RNA solution was added to each well containing ligand. This subsequent dilution lowered the final RNA concentration to 5 nM. To study the temperature dependence, the plates were incubated after overnight equilibrium at different temperature ranging from 5°C to 35°C.

Data analysis: Binding data (K_D and FRET experiments) were analyzed using Prism 5 (GraphPad Software) by nonlinear regression following the equation:

$$Y = \text{Bottom} + (\text{Top} - \text{Bottom})/(1 + 10^{[(\text{LogIC50-X})\text{xHillSlope}]})$$

K_D values were converted to $\Delta G°$ values as $\Delta G° = -RT\ln K_D$. Binding data were analyzed using the nonlinear least squares numerical solver-based binding data global analysis program GraphPad, in which the calculated binding surface is obtained using a numerical constrained optimization chemical equilibrium solver. Unless otherwise stated, binding profiles were well modeled using a simple model assuming the one to one stoichiometry. A higher initial fluorescence value is observed in the presence of tRNA, which is consistent with the modification of the polarity of the solvent and a small fluorescence of the tRNA mixture.

14

For thermodynamic analysis, $\Delta G°$ values were plotted versus T for the three-parameter fit5. Nonlinear regression in Prism 4 (GraphPad Software) was used to fit the following equation:

$$\Delta G°_T = \Delta H°_{Tr} + \Delta C_P (T - Tr) - T\Delta S°_{Tr} - T\Delta C_P \ln (T/Tr)$$

where Tr is a constant reference temperature (in our study Tr = 293.15 K), and the three fit parameters are $\Delta H°_{Tr}$, the change in enthalpy upon binding at Tr; $\Delta S°_{Tr}$, the change in entropy upon binding at Tr; and ΔC_P, the change in heat capacity. Starting values for the three parameters did not affect the final values. ΔC_P was assumed to be independent of temperature; inclusion of a $\Delta C_P/\Delta T$ term in the analysis did not improve the quality of the fits and gave larger standard errors for the returned parameters.

$\Delta H°_T$ and $\Delta S°_T$ were calculated by using:

$$\Delta H°_T = \Delta H°_{Tr} + \Delta C_P (T - Tr) \text{ and } \Delta S°_T = \Delta S°_{Tr} + \Delta C_P \ln (T/Tr).$$

Salt dependence of K_D was analyzed by the following equation:

$$\log(K_D) = \log(K_{nel}) - Z\psi \log [KCl]$$

where K_{nel} is the dissociation constant at the standard state in 1 M KCl, Z is the number of ions displaced from the nucleic acid (essentially the number of intermolecular ion pairs) and ψ is the fractional probability of a counterion being thermodynamically associated with each phosphate of the RNA number of cations. K_{nel} and $Z\psi$ were treated as fitting parameters.

Keywords

RNA ligands, TAR RNA, Verapamil, inhibition, RNA binding

Figures and Schemes

Figure 1. A) Primary and secondary structure of HIV-1 TAR RNA in complex with Tat, Cyclin T_1 and CDK9. Residues 18-44 that were used in this study are indicated; B) chemical structure of Verapamil.

Figure 2. K_D values (●) of compounds **2a-i**, **3a-i** and **5a-c** against HIV1 TAR RNA 27-mer fragment labeled at the 5'-end with Alexa[488]. Selectivity for TAR in the presence of 100 eq. of tRNA (■) and of DNA (▲) is reported. KD values were determined from duplicates performed over three independent experiments using the change in fluorescence intensity. Error bars represent the standard deviation determined from three independent experiments.

Figure 3. A) and B) Stacked plot of 1D NMR spectra of the imino region of 50 μM TAR RNA with increasing concentration of **1** (A) and **2h** (B). The spectra were collected at 286K in a H_2O/D_2O (90/10) buffer (20mM phosphate and 50mM NaCl, pH 7.4). C) and D) 2D-TOCSY spectra showing pyrimidine H5–H6 cross-peaks for TAR. Black: free TAR (100 μM); red: **1** (C) or **2h** (D)/TAR complex at a ratio 5:1. Arrows indicate chemical shift changes on ligand binding. The spectra were acquired at 308K in a D_2O buffer (50mM NaCl, 20mM phosphate, pH 7.4); E) and F) 27-mer TAR RNA primary and secondary structure illustrating the nucleotides that are the most affected by the presence of **1** (E) or **2h** (F).

Figure 4. Docking of **1** (A) and **2h** (B) with the 27-mer TAR hairpin loop performed by using autodock 4, in which the grid boxes were fixed on the entire RNA sequence.

Scheme 1. Synthetic procedure for the preparation of reduced verapamil **1** as well as of reductive amination products **2a-i**. Reagents: a) LiAlH$_4$, THF, 60°C, overnight; b) aldehyde, NaBH$_3$CN, CH$_2$Cl$_2$, r.t., overnight; c) TFA, CH$_2$Cl$_2$, r.t., overnight.

Scheme 2. Synthesis of amide-linked conjugates **3a-i**. Reagents: a) carboxylic acid, HBTU, DIPEA, CH$_2$Cl$_2$, r.t., overnight; b) TFA, CH$_2$Cl$_2$, r.t., overnight.

Scheme 3. Synthetic procedure for the synthesis of compound **4** bearing a succinamic acid linker and of amide-linked derivatives **5a-c**. Reagents: a) succinic anhydride, CH$_2$Cl$_2$, r.t., overnight; b) amine, HOBt, EDC, Et$_3$N, CH$_2$Cl$_2$, r.t., overnight; c) TFA, CH$_2$Cl$_2$, r.t., overnight.

16
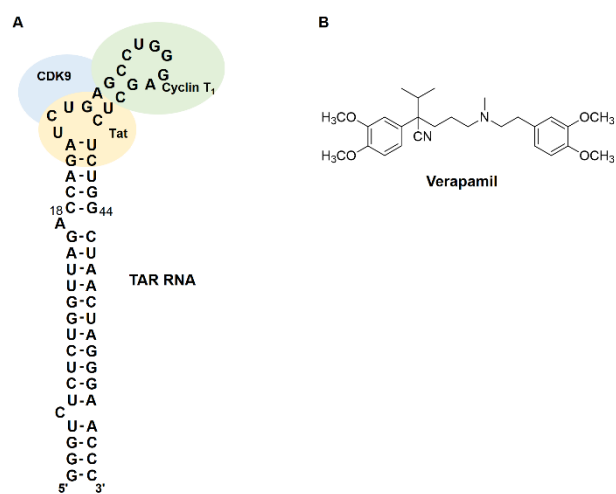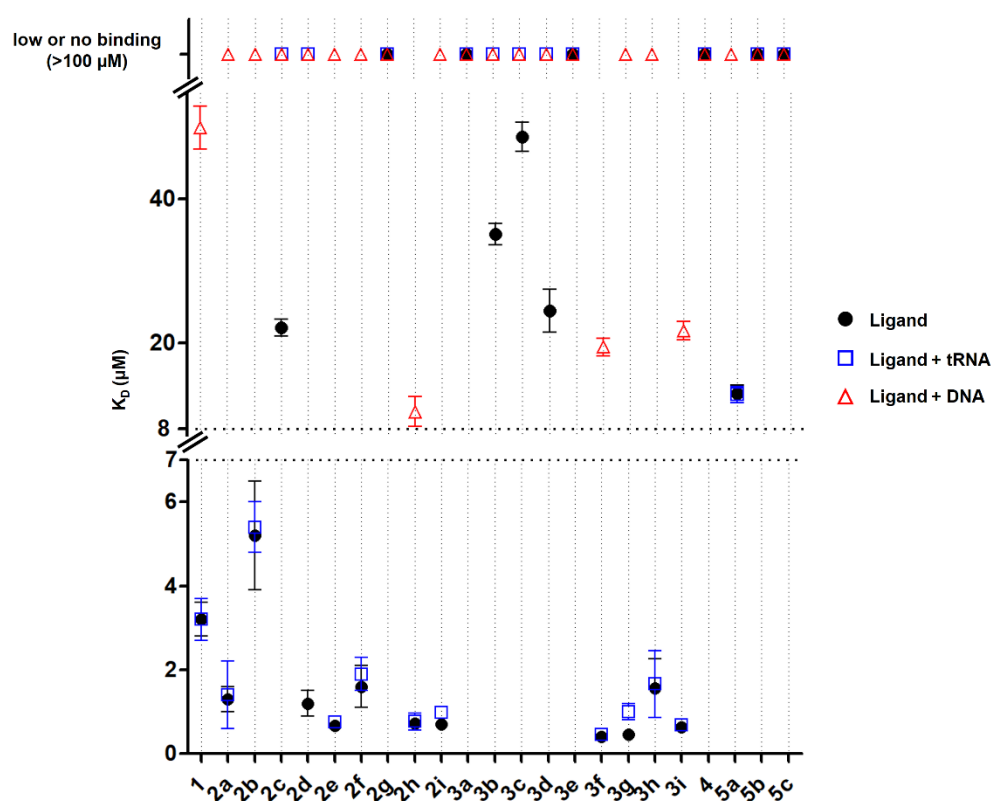
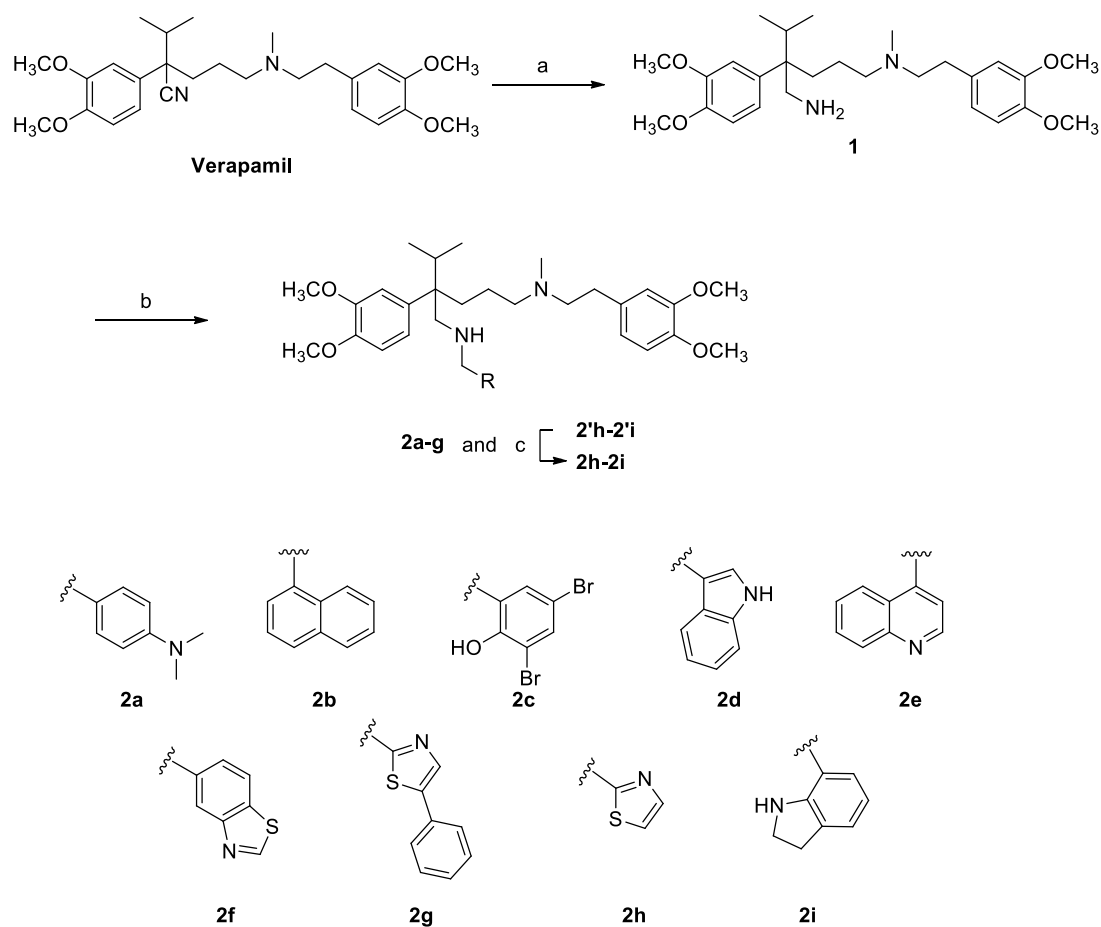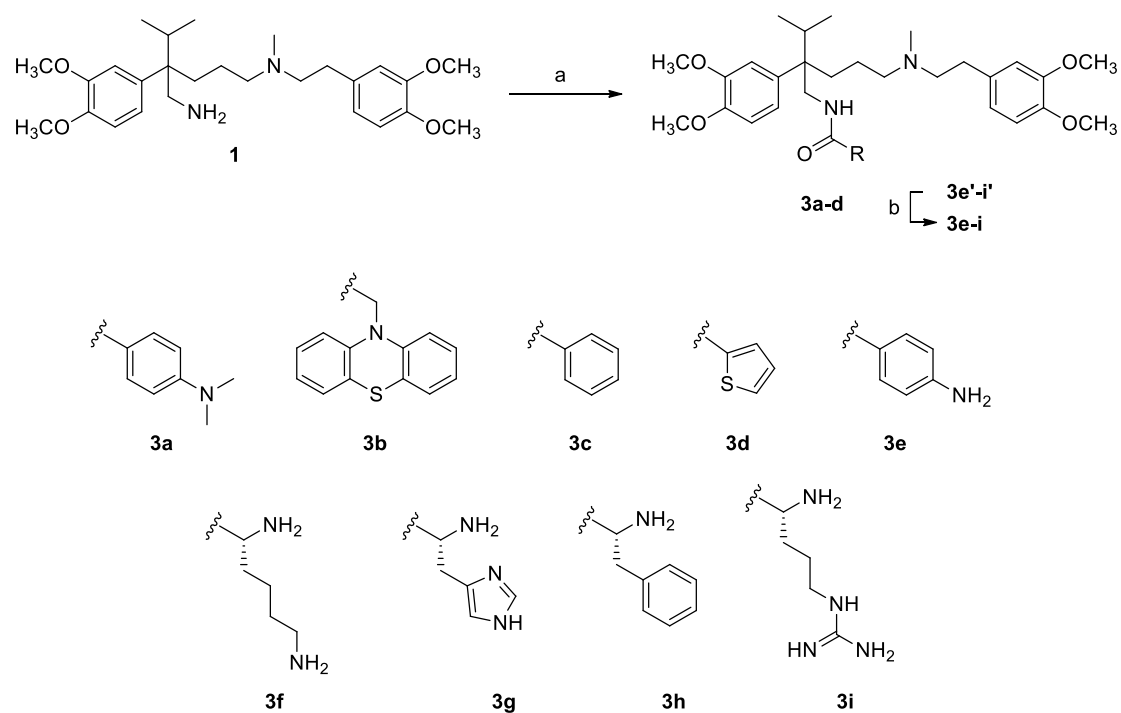**Figure 1**

Figure 2.

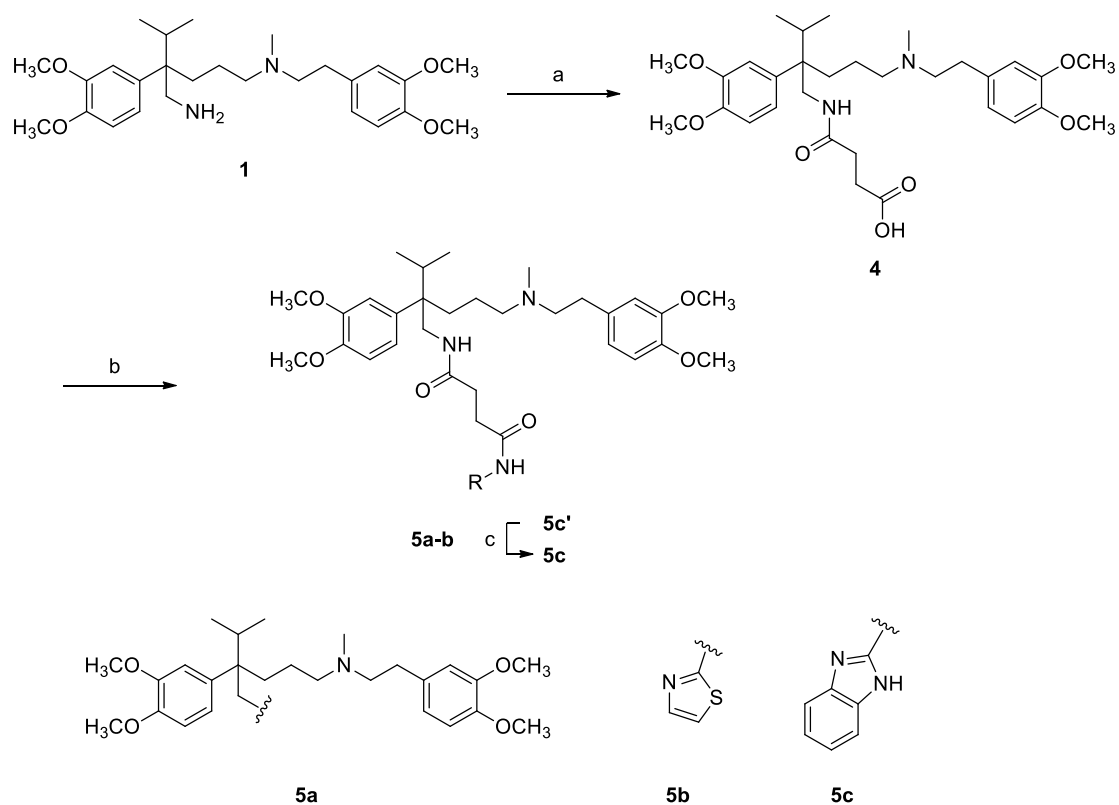**Figure 3.**
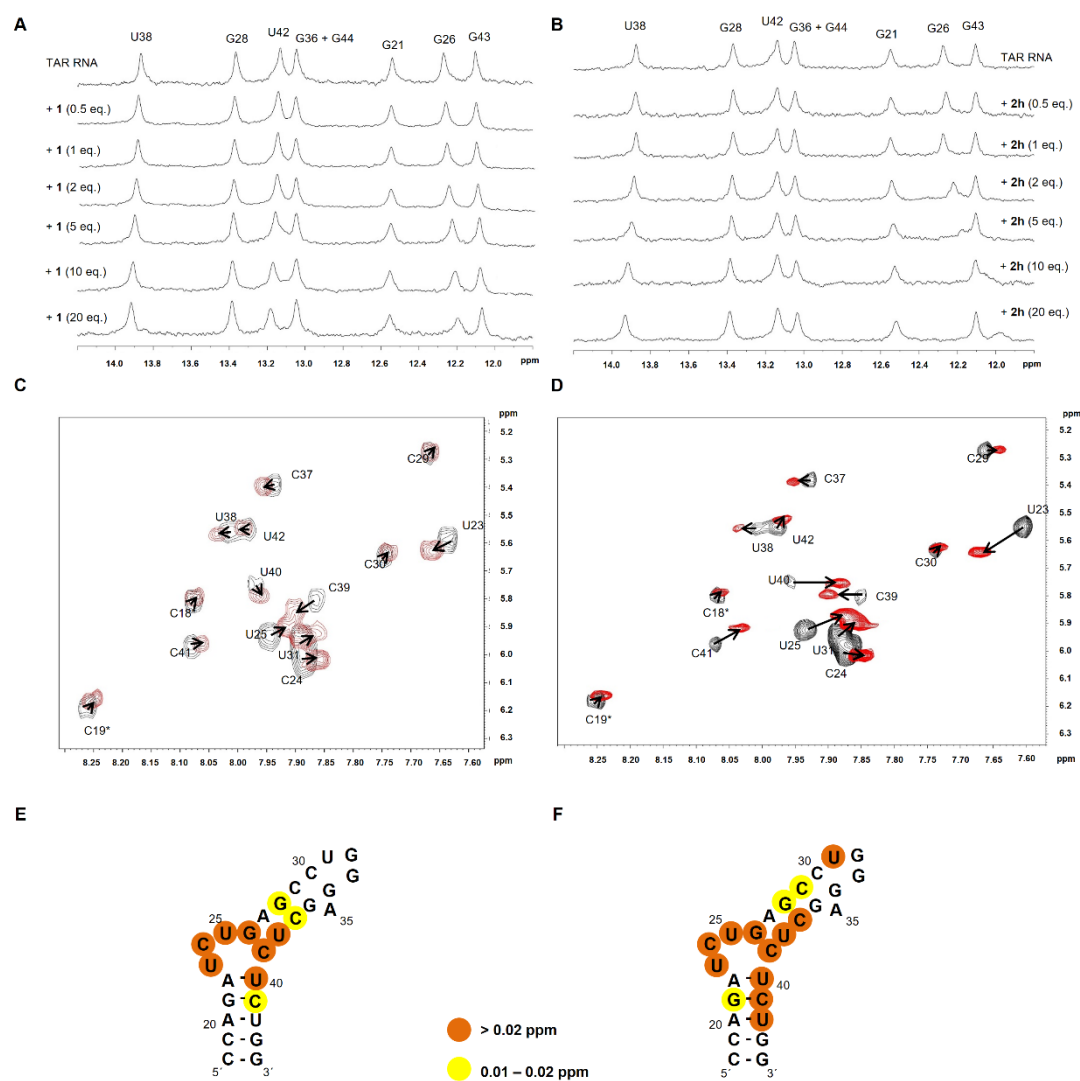
Figure 4.
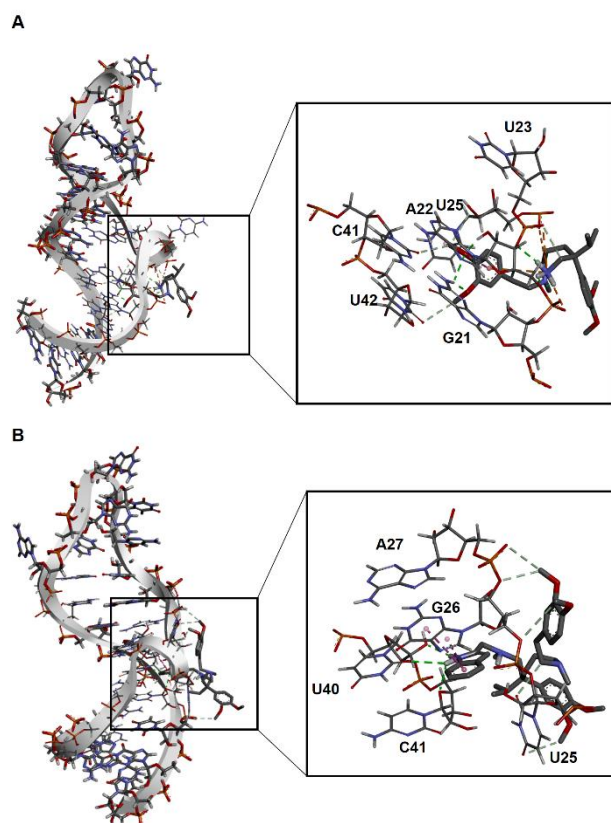
Scheme 1.

Scheme 2.

Scheme 3.

Table 1. Thermodynamic parameters for ligands/TAR RNA interaction and IC_{50} for the inhibition of Tat/TAR interaction.

ID	$\Delta G°$ (kJmol^{-1})	$\Delta H°$[a] (kJmol^{-1})	$T\Delta S°$[a] (kJmol^{-1})	$\Delta G°_{nel}$[b] (kJmol^{-1})	IC_{50} (μM)
1	-32.1 ± 2.7	-50.5 ± 4.7	-18.4 ± 1.2	-28.8 (90%)	1870 ± 12
2a	-32.6 ± 1.8	-16.1 ± 1.2	16.5 ± 1.5	not determined	no inhibition
2h	-34.8 ± 3.1	-33.3 ± 1.6	1.5 ± 1.0	-34.4 (99%)	18.8 ± 1.1
3f	-36.5 ± 3.1	-35.1 ± 2.9	1.4 ± 1.0	-32.8 (90%)	302 ± 5
3i	-36.0 ± 3.2	-24.2 ± 2.1	11.8 ± 1.2	-35.0 (97%)	404 ± 7

[a] Determined by temperature effect experiments by using the equation $\Delta G°_T = \Delta H°_{Tr} + \Delta C_P \cdot (T-Tr) - T\Delta S°_{Tr} - T\Delta C_P \ln(T/Tr)$. See the Supporting Information for definitions and further details. [b] Determined by salt effect experiments by using the equation $\log(K_D) = \log(K_{nel}) - ZY\log[KCl]$. See the Supporting Information for definitions and further details. The percentage of non-electrostatic interactions ($\Delta G°_{nel}/\Delta G°$) is given in parentheses.

24

[1]   a) A. Di Giorgio, M. Duca, *MedChemComm* **2019**, *10*, 1242-1255; b) M. D. Disney, *J Am Chem Soc* **2019**, *141*, 6776-6790; c) A. Donlic, A. E. Hargrove, *Wiley Interdiscip. Rev.: RNA* **2018**, *9*, e1477; d) K. D. Warner, C. E. Hajdin, K. M. Weeks, *Nat. Rev. Drug Discovery* **2018**, *17*, 547-558.

[2]   M. Matsui, D. R. Corey, *Nat. Rev. Drug Discovery* **2017**, *16*, 167-179.

[3]   E. Valeur, P. Jimonet, *J. Med. Chem.* **2018**, *61*, 9004-9029.

[4]   D. N. Wilson, *Nat. Rev. Microbiol.* **2014**, *12*, 35-48.

[5]   T. Hermann, *Wiley Interdiscip. Rev.: RNA* **2016**, *7*, 726-743.

[6]   A. Blond, E. Ennifar, C. Tisne, L. Micouin, *ChemMedChem* **2014**, *9*, 1982-1996.

[7]   M. Stevens, E. De Clercq, J. Balzarini, *Med. Res. Rev.* **2006**, *26*, 595-625.

[8]   K. S. Long, D. M. Crothers, *Biochemistry* **1995**, *34*, 8885-8895.

[9]   a) S. Kumar, P. Kellish, W. E. Robinson, Jr., D. Wang, D. H. Appella, D. P. Arya, *Biochemistry* **2012**, *51*, 2331-2347; b) S. Kumar, N. Ranjan, P. Kellish, C. Gong, D. Watkins, D. P. Arya, *Org. Biomol. Chem.* **2016**, *14*, 2052-2056; c) N. N. Patwardhan, L. R. Ganser, G. J. Kapral, C. S. Eubanks, J. Lee, B. Sathyamoorthy, H. M. Al-Hashimi, A. E. Hargrove, *MedChemComm* **2017**, *8*, 1022-1036; d) J. Sztuba-Solinska, S. R. Shenoy, P. Gareiss, L. R. Krumpe, S. F. Le Grice, B. R. O'Keefe, J. S. Schneekloth, Jr., *J. Am. Chem. Soc.* **2014**, *136*, 8402-8410; e) M. Zeiger, S. Stark, E. Kalden, B. Ackermann, J. Ferner, U. Scheffer, F. Shoja-Bazargani, V. Erdel, H. Schwalbe, M. W. Gobel, *Bioorg. Med. Chem. Lett.* **2014**, *24*, 5576-5580.

[10]   a) M. D. Disney, A. M. Winkelsas, S. P. Velagapudi, M. Southern, M. Fallahi, J. L. Childs-Disney, *ACS Chem. Biol.* **2016**, *11*, 1720-1728; b) C. S. Eubanks, B. Zhao, N. N. Patwardhan, R. D. Thompson, Q. Zhang, A. E. Hargrove, *J. Am. Chem. Soc.* **2019**, *141*, 5692-5698; c) B. S. Morgan, J. E. Forte, R. N. Culver, Y. Zhang, A. E. Hargrove, *Angew. Chem. Int. Ed.* **2017**, *56*, 13498-13502; d) B. S. Morgan, J. E. Forte, A. E. Hargrove, *Nucleic Acids Res.* **2018**, *46*, 8025-8037.

[11]   a) J. Palacino, S. E. Swalley, C. Song, A. K. Cheung, L. Shu, X. Zhang, M. Van Hoosear, Y. Shin, D. N. Chin, C. G. Keller, M. Beibel, N. A. Renaud, T. M. Smith, M. Salcius, X. Shi, M. Hild, R. Servais, M. Jain, L. Deng, C. Bullock, M. McLellan, S. Schuierer, L. Murphy, M. J. Blommers, C. Blaustein, F. Berenshteyn, A. Lacoste, J. R. Thomas, G. Roma, G. A. Michaud, B. S. Tseng, J. A. Porter, V. E. Myer, J. A. Tallarico, L. G. Hamann, D. Curtis, M. C. Fishman, W. F. Dietrich, N. A. Dales, R. Sivasankaran, *Nat. Chem. Biol.* **2015**, *11*, 511-517; b) H. Ratni, M. Ebeling, J. Baird, S. Bendels, J. Bylund, K. S. Chen, N. Denk, Z. Feng, L. Green, M. Guerard, P. Jablonski, B. Jacobsen, O. Khwaja, H. Kletzl, C. P. Ko, S. Kustermann, A. Marquet, F. Metzger, B. Mueller, N. A. Naryshkin, S. V. Paushkin, E. Pinard, A. Poirier, M. Reutlinger, M. Weetall, A. Zeller, X. Zhao, L. Mueller, *J. Med. Chem.* **2018**, *61*, 6501-6517; c) M. Sivaramakrishnan, K. D. McCarthy, S. Campagne, S. Huber, S. Meier, A. Augustin, T. Heckel, H. Meistermann, M. N. Hug, P. Birrer, A. Moursy, S. Khawaja, R. Schmucki, N. Berntenis, N.

Giroud, S. Golling, M. Tzouros, B. Banfai, G. Duran-Pacheco, J. Lamerz, Y. Hsiu Liu, T. Luebbers, H. Ratni, M. Ebeling, A. Clery, S. Paushkin, A. R. Krainer, F. H. Allain, F. Metzger, *Nat. Commun.* **2017**, *8*, 1476.

[12]   a) C. L. Haga, S. P. Velagapudi, J. R. Strivelli, W. Y. Yang, M. D. Disney, D. G. Phinney, *ACS Chem. Biol.* **2015**, *10*, 2267-2276; b) S. P. Velagapudi, M. D. Cameron, C. L. Haga, L. H. Rosenberg, M. Lafitte, D. R. Duckett, D. G. Phinney, M. D. Disney, *Proc. Natl. Acad. Sci. USA* **2016**, *113*, 5898-5903; c) S. P. Velagapudi, S. M. Gallo, M. D. Disney, *Nat. Chem. Biol.* **2014**, *10*, 291-297.

[13]   M. D. Disney, A. J. Angelbello, *Acc. Chem. Res.* **2016**, *49*, 2698-2704.

[14]   a) D. D. Vo, C. Becquart, T. P. A. Tran, A. Di Giorgio, F. Darfeuille, C. Staedel, M. Duca, *Org. Biomol. Chem.* **2018**, *16*, 6262-6274; b) D. D. Vo, M. Duca, *Methods Mol. Biol.* **2017**, *1517*, 137-154; c) D. D. Vo, C. Staedel, L. Zehnacker, R. Benhida, F. Darfeuille, M. Duca, *ACS Chem. Biol.* **2014**, *9*, 711-721; d) D. D. Vo, T. P. Tran, C. Staedel, R. Benhida, F. Darfeuille, A. Di Giorgio, M. Duca, *Chem. Eur. J.* **2016**, *22*, 5350-5362.

[15]   J. P. Joly, G. Mata, P. Eldin, L. Briant, F. Fontaine-Vive, M. Duca, R. Benhida, *Chem. Eur. J.* **2014**, *20*, 2071-2079.

[16]   J. P. Joly, M. Gaysinski, L. Zara, M. Duca, R. Benhida, *Chem. Commun.* **2019**, *55*, 10432-10435.

[17]   a) C. Becquart, M. Le Roch, S. Azoulay, P. Uriac, A. Di Giorgio, M. Duca, *ACS Omega* **2018**, *3*, 16500-16508; b) C. Staedel, T. P. A. Tran, J. Giraud, F. Darfeuille, A. Di Giorgio, N. J. Tourasse, F. Salin, P. Uriac, M. Duca, *Sci. Rep.* **2018**, *8*, 1667.

[18]   a) N. W. Luedtke, Q. Liu, Y. Tor, *Biochemistry* **2003**, *42*, 11391-11403; b) A. C. Stelzer, A. T. Frank, J. D. Kratz, M. D. Swanson, M. J. Gonzalez-Hernandez, J. Lee, I. Andricioaei, D. M. Markovitz, H. M. Al-Hashimi, *Nat. Chem. Biol.* **2011**, *7*, 553-559; c) J. R. Thomas, P. J. Hergenrother, *Chem. Rev.* **2008**, *108*, 1171-1224.

[19]   D. A. Erlanson, B. J. Davis, W. Jahnke, *Cell Chem. Biol.* **2019**, *26*, 9-15.

[20]   J. R. Thomas, X. Liu, P. J. Hergenrother, *J. Am. Chem. Soc.* **2005**, *127*, 12434-12435.

[21]   M. Mayer, P. T. Lang, S. Gerber, P. B. Madrid, I. G. Pinto, R. K. Guy, T. L. James, *Chem. Biol.* **2006**, *13*, 993-1000.

[22]   K. F. Blount, Y. Tor, *ChemBioChem* **2006**, *7*, 1612-1621.

[23]   a) B. Bognar, S. Ahmed, M. L. Kuppusamy, K. Selvendiran, M. Khan, J. Jeko, O. H. Hankovszky, T. Kalai, P. Kuppusamy, K. Hideg, *Bioorg. Med. Chem.* **2010**, *18*, 2954-2963; b) L. J. Theodore, W. L. Nelson, R. H. Zobrist, K. M. Giacomini, J. C. Giacomini, *J. Med. Chem.* **1986**, *29*, 1789-1792.

[24]   a) G. Klebe, *Nat. Rev. Drug Discovery* **2015**, *14*, 95-110; b) A. Umuhire Juru, N. N. Patwardhan, A. E. Hargrove, *ACS Chem. Biol.* **2019**, *14*, 824-838.

[25]   A. I. Murchie, B. Davis, C. Isel, M. Afshar, M. J. Drysdale, J. Bower, A. J. Potter, I. D. Starkey, T. M. Swarbrick, S. Mirza, C. D. Prescott, P. Vaglio, F. Aboul-ela, J. Karn, *J. Mol. Biol.* **2004**, *336*, 625-638.

[26]   L. Pascale, A. L. Gonzalez, A. Di Giorgio, M. Gaysinski, J. Teixido Closa, R. E. Tejedor, S. Azoulay, N. Patino, *J. Biomol. Struct. Dyn.* **2016**, *34*, 2327-2338.

[27]   T. P. Tran, D. D. Vo, A. Di Giorgio, M. Duca, *Bioorg. Med. Chem.* **2015**, *23*, 5334-5344.

[28]   L. Pascale, S. Azoulay, A. Di Giorgio, L. Zenacker, M. Gaysinski, P. Clayette, N. Patino, *Nucleic Acids Res.* **2013**, *41*, 5851-5863.

27